Carbon nanotube-based quantum pump in the presence of superconducting lead

Yadong Wei[1] and Jian Wang[2,a)]
1. Department of Physics, School of Science, Shenzhen University, Shenzhen 518060, China
2. Department of Physics, The University of Hong Kong, Pokfulam Road, Hong Kong, China

Parametric electron pump through superconductor-carbon-nanotube based molecular devices was investigated. It is found that a dc current, which is assisted by resonant Andreev reflection, can be pumped out from such molecular device by a cyclic variation of two gate voltages near the nanotube. The pumped current can be either positive or negative under different system parameters. Due to the Andreev reflection, the pumped current has the double peak structure around the resonant point. The ratio of pumped current of N-SWNT-S system to that of N-SWNT-N system (I^{NS}/I^{N}) is found to approach four in the weak pumping regime near the resonance when there is exactly one resonant level at Fermi energy inside the energy gap. Numerical results confirm that in the weak pumping regime the pumped current is proportional to the square of the pumping amplitude V_p, but in the strong pumping regime the pumped current has the linear relation with V_p. Our numerical results also predict that pumped current can be obtained more easily by using zigzag tube than by using armchair tube.

73.63.Fg,85.35.Kt,73.40.Gk,74.50.+r

I. INTRODUCTION

Physics of parametric electron pump has attracted great attention. Classical pumps had been fabricated about a decade ago[1,2]. Recently, Quantum-dot-based quantum pump has been the subject of both experimental[3] and theoretical[4–20] investigations. The quantum pump generates current due to the cyclic variation of at least two system parameters while maintaining zero bias. As the charge pumped out of the system, it also produces the Joule heat along with the dissipation. Recently, Avron et al[21] have derived the lower bound for the dissipation. This naturally leads to the concept of optimal pump. To search for an optimal pump, the heat current and the shot noise of quantum pump have been investigated using the time-dependent scattering matrix theory[22–24]. Very recently, to explain the experimentally observed anomaly[3], the finite frequency pumping theory has been developed[25,26]. The adiabatic pumping theory has also been extended to account for the Andreev reflection in the presence of superconducting lead[18,27], strong electron interaction in the Kondo regime[28], and spin polarized pumped current when the ferromagnetic leads are present[29]. Due to the peculiar electronic properties of Carbon nanotube (CNT)[30–38], CNT-based parametric electron pump has been investigated as a prototypical nanometer-scale molecular device[14]. It would be interesting to further explore how does Andreev reflection modify the quantum interference of CNT based quantum pump in the presence of superconducting lead. It is well known that in the presence of normal conductor-superconductor (NS) interface, an incoming electron-like excitation can be Andreev reflected as a hole-like excitation[39]. In this paper, we will study a hybrid structure where both carbon nanotube and superconducting lead are present and examine the interplay between the electronic properties of CNT and superconductivity. Specifically, we investigate a parametric quantum pump that consists of a finite sized single wall carbon nanotube (SWNT) connected to one normal left lead (N) and one superconducting right lead (S), i.e., the parametric quantum pump of N-SWNT-S system. Two pumping driving forces $X_1(t)$ and $X_2(t)$ are established by applying cyclic, time-dependent voltages to two metallic gates, which are capacitively coupled to the SWNT (see inset of Fig.1). We have used nonequilibrium Green's function approach[40–42] to calculate the pumped current. We found that in the presence of superconducting lead the pumped current is four times as that of corresponding normal system in the weak pumping regime. As the pumping amplitude increases, the de-

pendence of pumped current crosses over from quadratic to the linear dependence. Due to the Andreev reflection, the pumped current exhibits double peak structure for single resonant level in line with the chemical potential μ_s of the superconducting lead. When μ_s is in the middle of two resonant levels, another type of Andreev reflection occurs where an electron coming from normal lead tunnels via the lower resonant level and Andreev reflected as a hole through the upper resonant level with a Cooper pair created in the superconducting lead. For this two level Andreev reflection, the pumped current shows remarkable parity effect that the direction of pumped current near one resonant level is opposite to that of the other level. Finally, our numerical results show that it is much easier to pump current through zigzag structure than armchair structure.

II. THEORY

In this work, we assume that the variation of the pumping potentials are very slow and the adiabatic approximation is appropriate. In this approximation, the pumped current flowing through the left normal metallic lead, in one cycle time τ, is given by[4,18,43]

$$I^{NS} = \frac{q\omega}{2\pi}\int_0^\tau d\tau[\frac{dN_L}{dX_1}\frac{dX_1}{dt} + \frac{dN_L}{dX_2}\frac{dX_2}{dt}] \tag{1}$$

where the quantity dN_L/dX_j is the partial density of states (DOS), called the injectivity[44,45], of the left lead

$$\frac{dN_L}{dX_j} = \frac{dN_L^e}{dX_j} - \frac{dN_L^h}{dX_j} \tag{2}$$

with

$$\frac{dN_L^e}{dX_j} = -\int\frac{dE}{2\pi}(-\partial_E f)Tr[G_{11}^r\Gamma_L G_{11}^a\Delta_j] \tag{3}$$

and

$$\frac{dN_L^h}{dX_j} = -\int\frac{dE}{2\pi}(-\partial_E f)Tr[G_{12}^r\Gamma_L G_{12}^a\Delta_j] \tag{4}$$

where $j = 1$ or 2. dN_L^e/dX_j describes the number of electrons coming from left lead and exiting the system as electrons due to the external parameter X_j. dN_L^h/dX_j describes the number of holes coming from left lead and exiting the system as electrons due to the external parameter X_j[45]. G_{11} and G_{12} are the matrix elements of the 2×2 Nambu[46] representation and can be expressed as[47]:

$$G_{11}^r(E) = [E - H_d - V_{pp} - \mathbf{\Sigma}_{11}^r - \mathbf{\Sigma}_{12}^r A^r \mathbf{\Sigma}_{21}^r]^{-1} \tag{5}$$

and

$$A^r = [E + H_d + V_{pp} - \mathbf{\Sigma}_{22}^r]^{-1} \tag{6}$$

Once the electron and hole Green's function G_{11}^r and A^r were obtained, G_{12}^r is calculated by

$$G_{12}^r = G_{11}^r\mathbf{\Sigma}_{12}^r A^r \tag{7}$$

Here $\Gamma_{L,R} = -2Im[\Sigma_{L,R}^r]$ is the line-width function and $\mathbf{\Sigma}^r = \mathbf{\Sigma}_L^r + \mathbf{\Sigma}_R^r$ is the total self energy given by

$$\mathbf{\Sigma}_L^r = \begin{pmatrix} \Sigma_L^r & 0 \\ 0 & -\Sigma_L^a \end{pmatrix} \tag{8}$$

where $\Sigma_\alpha^r \equiv P_\alpha - i\Gamma_\alpha/2$ is the self energy of the lead α in the normal case. Here P_α is the real part and Γ_α is the linewidth function. The self energy for the superconducting lead is

$$\mathbf{\Sigma}_R^r = \begin{pmatrix} P_R - i\Gamma_R\beta_1/2 & i\Gamma_R\beta_2/2 \\ i\Gamma_R\beta_2/2 & -P_R - i\Gamma_R\beta_1/2 \end{pmatrix} \tag{9}$$

where $\beta_1 = \nu E/\sqrt{E^2-\Delta^2}$, $\beta_2 = \nu\Delta/\sqrt{E^2-\Delta^2}$ with $\nu = 1$ for $E > -\Delta$ and $\nu = -1$ for $E < -\Delta$. Here Δ is the gap energy of superconducting lead and chemical potential of superconducting lead μ_s has been set to zero. In the above equations, H_d is the Hamiltonian of CNT. It is a $N\times N$ matrix, where N is the total number of carbon atoms. V_{pp} is a diagonal matrix describing the variation of the CNT potential landscape due to the external pumping potentials $X_1(t)$ and $X_2(t)$. In this work, we choose the two pumping potentials to be $X_1(t) \equiv V_1(t) = V_{10} + V_{1p}\sin(\omega t)$ and $X_2(t) \equiv V_2(t) = V_{20} + V_{2p}\sin(\omega t + \phi)$, where ϕ is phase difference, ω is the pumping frequency and V_{1p} and V_{2p} are the pumping amplitudes. To simplify the numerical calculation, we mimic the gate effects by simply adding the potential $V_{pp} = V_1\Delta_1 + V_2\Delta_2$ to the SWNT where Δ_i is the potential profile function and can be set to be unit for the gate region, zero otherwise. A more accurate study requires a numerical solution of the Poisson equation with the gates providing the appropriate boundary conditions.

III. RESULT AND DISCUSSION

We now apply Eq.(1) to calculate the current for the N-SWNT-S parametric pump. For simplicity, the SWNT is modeled with the nearest neighbor π-orbital tight-binding model with bond potential $V_{pp\pi} = -2.75$eV. This model gives a reasonable, qualitative description of the electronic and transport properties of carbon nanotubes[48,49]. Recently, a S-SWNT-S device has been studied experimentally[34]. By tuning the transparency of the device, clear signals of Andreev reflection were observed. The dependence of the Andreev current on the device transparency, the behavior of the differential resistance in the sub-gap region, as well as the observed low-temperature resistance anomaly[34] can all be explained theoretically using the π-orbital tight-binding

model[50]. We assume that the SWNT is weakly coupled to the electrodes so that the pumping process is mediated by the resonant tunneling. We further assume that strong electron-electron interactions may be neglected. Without losing generality, we set the energy gap of the superconducting lead to be $1.45meV$ (the gap of Niobium). We also apply the wide bandwidth limit for the self-energy[40] and consider the symmetric pumping, i.e., $V_{10} = V_{20} = V_0$ and $V_{1p} = V_{2p} = V_p$. In the absence of pumping we have $V_p = 0$ which forms a symmetric double barrier with barrier height V_0 in the finite size nanotube. As a result, the discrete resonant levels are established within the double barrier structure. By adjusting V_0, we can control the positions of energy levels inside the energy gap Δ. Since the pumped current is proportional to ω, we set $\omega = 1$ for convenience. We also set $\hbar = 2m = e = 1$. When pumping frequency $\omega = 100MHz$, which is close to the frequency used in Ref. 3, the unit for the pumped current is 1.6×10^{-11}A. Finally, we do not consider the finite temperature effect and hence set temperature to zero.

First, we consider an armchair (5,5) SWNT with 93 layers of carbon atoms (total 930 atoms). The two metallic gates that provide the pumping driving forces are located near the two ends of the SWNT from 10th to 28th layer, and 66th to 84th layer. We have chosen $V_0 \approx 2.75V$ so that there is only one resonant level in the energy gap and the level is aligned with the chemical potential of the superconducting lead in the absence of pumping voltage $V_p = 0$. Fig.1 shows the transmission coefficient versus Fermi energy E_F. For comparison, the transmission coefficient for corresponding normal system (when $\Delta = 0$) is also plotted. We see that for normal system, the transmission coefficient (dashed line) has Lorentzian lineshape. In the presence of superconducting lead, the transmission peak (solid line) is flattened and narrowed. Fig.2 depicts the pumped current I^{NS} versus the Fermi energy for different pumping amplitudes V_p with $\phi = \pi/2$ and $\Gamma_L = \Gamma_R = 0.0136eV$. Several interesting observations are in order. (1). the pumped current has large amplitude only near the resonant level showing clearly a resonant assisting behavior. This is because the pumped current is related to the global density of states (DOS) and the DOS of the system reaches its maximum near the resonant level[8]. (2). the amplitude of pumped current has double-peak structure around the resonant level. To understand this behavior, we plot the Andreev reflection coefficient versus E_F at different times t during the pumping cycle in the right inset of Fig.2. The Andreev reflection coefficient gives large value only around the two pumping instants: $t = 3\pi/4$ and $t = 7\pi/4$ because at such moments the energy level of the SWNT is just in line with the chemical potential of the superconducting lead so that an excitation of hole can be reflected when there is an incident election near the Fermi surface, and vice verse. At other moments, Andreev reflection coefficient is very small and contributes little to the current integral in the time cycle. In the inset, we just plot Andreev coefficients at certain moments: $t_0 = 3\pi/4$, $t_0 = 0.95 \times 3\pi/4$ (a little smaller than t_0) and $t_0 = 1.05 \times 3\pi/4$ (a little lager than t_0). We see that all three curves have double-peak feature (for the solid line the double-peak is barely seen). To understand this, we examine the Andreev reflection coefficient which takes on the Breit-Wigner form near the resonant level E_0[50]:

$$T_A(E) = \frac{\Gamma_1^2\Gamma_2^2}{4\left[E^2 - E_o^2 + \frac{\Gamma\delta\Gamma}{4}\right]^2 + \Gamma_1^2\Gamma_2^2 + E_o^2\left[\Gamma + \delta\Gamma\right]^2}, \tag{10}$$

where $\delta\Gamma \equiv \Gamma_1 - \Gamma_2$ and $\Gamma = \Gamma_1 + \Gamma_2$. Here Γ_1 and Γ_2 are linewidth functions which characterize the ability of electron tunneling through the left and right barriers, respectively. At the moment $t_0 = 3\pi/4$, the barrier heights for the left and right barriers are $V_0 + (\sqrt{2}/2)V_p$ and $V_0 - (\sqrt{2}/2)V_p$, respectively. In this case, we found that the position of the resonant level remains the same as when $V_p = 0$, i.e., the resonant level is still at $E_0 = 0$. From Eq.(10), we have

$$T_A(E) = \frac{\Gamma_1^2\Gamma_2^2}{4\left(E^2 + \frac{\Gamma\delta\Gamma}{4}\right)^2 + \Gamma_1^2\Gamma_2^2}\ . \tag{11}$$

Eq.(11) indicates that if $\Gamma_1 = \Gamma_2$ so that $\delta\Gamma = 0$, then resonant Andreev reflection occurs at $E = 0$ with $T_A(E = 0) = 1$. On the other hand, if $\Gamma_1 > \Gamma_2$ so that $\delta\Gamma > 0$, T_A takes on a maximum value at $E = 0$ but this maximum value is less than 1. Furthermore, if $\Gamma_1 < \Gamma_2$ such that $\delta\Gamma < 0$, T_A is characterized by two resonant peaks with $T_A = 1$ at energies $E_\pm = \pm\sqrt{-\Gamma\delta\Gamma}/2$. Since the left barrier is higher than the right one, we have $\Gamma_1 < \Gamma_2$. This explains why we have double-peak feature for the solid curve in the right inset of Fig.2. At the moment $t_0 = 0.95 \times 3\pi/4$ or $t_0 = 1.05 \times 3\pi/4$, the resonant level shift so that E_0 is no longer zero. The double-peak structure can still be explained using Eq.(10). Similar discussions apply to the moment $t = 7\pi/4$. From the above discussion, it is clear that the double-peak feature of Andreev coefficient around $t_0 = 3\pi/4$ and $t_0 = 7\pi/4$ is responsible for the behavior of the pumped current. (3). the pumped current increases as the pumping amplitude V_p increases (compare solid line, dotted line, and dashed line in Fig.2). (4). For comparison, we also plot the pumped current I^N for N-SWNT-N system with $V_p = 0.0014V$ (long dashed line in Fig.2). We see that it gives only one broad peak with small magnitude rather than two peaks. This is because for normal system the transmission coefficient does not give two peaks at any pumping moment and the double-peak feature for transmission coefficient is the intrinsic feature solely due to the Andreev reflection at the NS interface. Due to the quantum interference between the direct reflection (with amplitude E_d) and the multiple Andreev reflection (amplitude E_A), the pumped current I^{NS} of N-SWNT-S is greatly enhanced and is much larger than the pumped

current I^N of the same system when the superconducting lead becomes normal[18]. Roughly speaking, we have $I^{NS} \sim |E_d + E_A \exp(i\theta)|^2$ where θ is the phase difference between E_d and E_A. In the right inset of Fig.2, we plot the ratio of I^{NS}/I^N as a function of pumping amplitude V_p at the resonant energy. At small pumping amplitude, the direct reflection and the multiple Andreev reflection are exactly in phase ($\theta = 0$) and the complete constructive interference gives the ratio around four[18]. As the pumping amplitude increases, the constructive interference effect in the N-SWNT-S system is suppressed because $\theta \neq 0$.

Now we consider a zigzag (10,0) SWNT with $L = 56$ layers of carbon atoms (total 560 atoms). Two pumping driving forces are added on the tube layers from 5th to 8th layer and from 49th to 52nd layer. By adjusting $V_0 \approx 2.10065V$, one resonant level is available at $E_F = 0$. In the calculation, we set $\phi = \pi/2$ and $\Gamma_R = \Gamma_L = 0.0136eV$. The results are plotted in Fig.3. We see that the pumped current gives similar behavior to that of armchair SWNT system. The pumped current is large near the resonant level and also has the double-peak structure around the resonant point. The ratio of I^{NS}/I^N is also about four in the weak pumping regime (see the inset of Fig.3). Moreover there are several points worth mentioning. First, the pumped current can either be positive or negative even for the same SWNT but different energy levels or different phase differences (see Fig.5 and Fig.6). Comparing with armchair structure, the pumped current for zigzag structure reverses the direction. This is because the pumped current is not due to the external bias but cause by the pumping potentials. As a result, the pumped current is very sensitive to the system parameters. Second, the double-peak for the pumped current is asymmetric especially when the pumping amplitude is large (see the dashed line of Fig.3). This is mainly due to the energy dependence of the self-energy. Third, under the same system parameters[51], the pumped current of zigzag structure is much larger (at least ten times larger) than that of armchair structure. This means that in order to obtained large pumped current, one should use zigzag nanotube instead of armchair nanotube. This may be useful for experimental study of the carbon nanotube pump.

Fig.4 gives the pumped current as a function of pumping amplitude V_p at $E_F = 0$ for armchair SWNT. Here the system parameters are the same as those in Fig.2. We see that the pumped current increases quadratically at small pumping amplitude and then reaches linear regime for large pumping amplitude. In order to understand this figure, we also plot $I = -1.06 \times 10^4 V_p^2$ in the same plot. We confirm that in the weak pumping regime the pumped current is proportional to the square of the pumping amplitude, but in the strong pumping regime the pumped current is linearly proportional to V_p only. Similar conclusion can be drawn from the zigzag nanotube (see the inset of Fig.4). Fig.5 and the inset of Fig.5 present the pumped currents of armchair SWNT versus phase difference at different pumping amplitudes in the weak pumping regime and the strong pumping regime, respectively. We see that the pumped current is anti-symmetric about $\phi = \pi$, just like the the result given by the experiments of Ref.[3] although superconducting lead was not used there. In the weak pumping regime, the sinusoidal behavior is clearly seen. In the strong pumping regime, however, we see strong deviation from the sinusoidal behavior (see inset of Fig.5) and the maximum pumped current occurs near $\phi = \pi$ instead of $\phi/2$.

Finally, we examine another N-SWNT-S quantum pump using a zigzag (10,0) tube with $L = 92$ layers (total atoms 920). One gate is located from 10th to 28th layer and the other is located from 65th to 83rd layer. By adjusting $V_0 \approx 2.5936V$, we obtain two double degenerated resonant levels at $E_1 = -3.5495 \times 10^{-5} eV$ and $E_2 = 3.5495 \times 10^{-5} eV$. Hence, large Andreev reflections can occur near $E_F = E_1$ and $E_F = E_2$ with transmission coefficient equals to two (see the upper panel of Fig.6). Here the Andreev reflection is due to different origin from that of Fig.1. In Fig.1, we have $E_0 = 0$ and Eq.(10) gives us the resonance at $E = 0$ with $T_A = 1$. If E_0 is nonzero the maximum Andreev reflection is less than one. In the strong tunneling regime which applies to our case, Γ_1 and Γ_2 are very small. To simplify the discussion, let us assume $\Gamma_1 = \Gamma_2 << 1$, then from Eq.(10), we have

$$T_A = \frac{\Gamma_1^4}{[4(E^2 - E_0^2)^2 + \Gamma_1^4 + 4E_0^2\Gamma_1^2]}$$

At resonance, $T_A = \Gamma_1^2/[\Gamma_1^2 + 4E_0^2]$. Hence when E_0 is larger than Γ_1, the Andreev reflection quickly goes to zero. However, if the chemical potential of the superconducting lead (μ_s=0 in our case) is right in the middle of two resonant levels (E_1 and E_2), *i.e.*, $\mu_s = (E_1 + E_2)/2$, then electron coming from normal lead with incident energy E_1 tunnels into the structure through the resonant level E_1 and Andreev reflected as a hole back to the quantum dot through the resonant level E_2 with a Copper pair created in the superconducting lead, giving rise to the complete transmission. This is why in the upper panel of Fig.6 we have two transmission peaks with $T_A = 2$ due to the double degeneracy. The pumped current as a function of Fermi energy is plotted in Fig.6. For comparison, we also plot the transmission coefficient (long dashed line for normal structure and solid line for NS structure) in the upper panel of Fig.6. The pumped current with $V_p = 1 \times 10^{-6} V$ (long dashed line in Fig.6) for the N-SWNT-N system with the same system parameters is also shown. Similar to Fig.2 and Fig.3, the pumped current also shows strong resonant behavior. It has large value near energies where the Andreev reflection peaks occur, while it diminishes quickly away from the peaks. The amplitude of pumped current also increases as the pumping amplitude V_p increases. The striking feature here is that the pumped current peaks have opposite sign for the two energy levels. That means the pump has property that the DC current can flow out of the

device from either electrodes by a slight change of electron energy. From the lower inset of Fig.6, we see that the pumped current clearly consists of two asymmetric peaks. Finally, we notice that large pumped current is generated for very small pumping amplitude (compare Fig.3 with Fig.6). This is because in Fig.6 the thickness of potential barrier and hence the effective potential barrier height is much higher than that in Fig.3. As shown in Ref. 11,52 that the maximum pumped current can reach $1/2\pi$ for extremely large barrier and in strong pumping regime.

In summary, we have investigated the parametric pump of N-SWNT-S systems. By comparing with the parametric pump of N-SWNT-N system, we find that in the presence of superconducting lead, the pumped currents is greatly enchanced due to the quantum interference of direct reflection and multiple Andreev reflection. In the weak pumping regime, the pumped current is proportional to the square of the pumping amplitudes but in the strong pumping regime, the dependence becomes linear. Hence large pumped current can be generated by increasing the pumping amplitude. When two level Andreev reflection occurs, the pumped current show remarkable parity effect so that the pumped current at one resonant level has opposite direction of that of the other resonant level. Our numerical results also show that the zigzag nanotube is a better candidate for the pumping device since it is more easily pumped than the armchair nanotube. In view of the S-SWNT-S structure studied in Ref. 34, it is conceivable that the N-SWNT-S quantum molecular pump can be realized experimentally and the results presented here be verified.

ACKNOWLEDGMENTS

We gratefully acknowledge support by a RGC grant from the SAR Government of Hong Kong under grant number HKU 7091/01P.

[a)] Electronic mail: jianwang@hkusub.hku.hk

[1] L.P. Kouwenhoven, *et.al.*, Phys. Rev. Lett. **67**, 1626 (1991).
[2] H. Pothier *et. al.*, Europhys. Lett. **17**, 249 (1992).
[3] M. Switkes, C. Marcus, K. Capman, and A.C. Gossard, Science **283**, 1905 (1999).
[4] P.W. Brouwer, Phys. Rev. B **58**, R10135 (1998).
[5] I.L. Aleiner and A.V. Andreev, Phys. Rev. Lett. **81**, 1286 (1998).
[6] F. Zhou, B. Spivak, and B.L. Altshuler, Phys. Rev. Lett. **82**, 608 (1999).
[7] T.A. Shutenko, I.L. Aleiner, and B.L. Altshuler, Phys. Rev. B **61**, 10366 (2000).
[8] Y.D. Wei, J. Wang, and H. Guo, Phys. Rev. B **62**, 9947 (2000).
[9] I.L. Aleiner, B.L. Altshuler, and A. Kamenev, Phys. Rev. B **62**, 10373 (2000).
[10] J.E. Avron, A. Elgart, G.M. Graf, and L. Sadun, Phys. Rev. B **62**, R10618 (2000).
[11] Y. Levinson, O. Entin-Wohlman, and P. Wolfle, Physica A **302**, 335 (2001).
[12] P.W. Brouwer, Phys. Rev. B **63**, 121303 (2001); M.L. Polianski and P.W. Brouwer, Phys. Rev. B **64**, 075304 (2001).
[13] M. Moskalets and M. Buttiker, Phys. Rev. B **64**, 201305 (2001).
[14] Y.D. Wei, J. Wang, H. Guo, and C. Roland, Phys. Rev. B **64**, 115321 (2001).
[15] F. Renzoni and T. Brandes, Phys. Rev. B **64**, 245301 (2001).
[16] Y. Makhlin and A.D. Mirlin, Phys. Rev. Lett. **87**, 276803 (2001).
[17] C.S. Tang and C.S. Chu, Solid State Comm. **120**, 353 (2001).
[18] J. Wang, Y.D. Wei, B.G. Wang, and H. Guo, Appl. Phys. Lett. **79**, 3977 (2001).
[19] O. Entin-Wohlman, A. Aharony, and Y. Levinson, preprint: cond-mat/0201073.
[20] O. Entin-Wolman and A. Aharony, cond-mat/0202289.
[21] J.E. Avron, A. Elgart, G.M. Graf, and L. Sadun, Phys. Rev. Lett. **87**, 236601 (2001).
[22] M. Moskalets and M. Buttiker, cond-mat/0201259.
[23] M.L. Polianski, M.G. Vavilov, and P.W. Brouwer, cond-mat/0202241.
[24] B.G. Wang and J. Wang, cond-mat/0204067.
[25] M.G. Vavilov, V. Ambegaokar, and I.L. Aleiner, Phys. Rev. B **63**, 195313 (2001).
[26] B.G. Wang, J. Wang, and H. Guo, Phys. Rev. B **65**, 073306 (2002).
[27] M. Blaauboer, cond-mat/0204340.
[28] B.G. Wang and J. Wang, Phys. Rev. B **65**, 233315 (2002).
[29] J.L. Wu, B.G. Wang, and J. Wang, cond-mat/0204570.
[30] Z. Yao, H.W.Ch. Postma, L. Balents and C. Dekker, Nature, **402**, 273 (1999).
[31] Kazuhito Tsukagoshi, Bruce W. Alphenaar and Hiroko Ago, Nature, **401**, 572 (1999).
[32] S.J. Tans, *et.al.* Nature, **386**, 174 (1997).
[33] S. Frank, P. Poncharal, Z. L. Wang, and W. A. de Heer,

Science, **280**, 1744 (1998).
[34] A.F. Morpurgo, J. Kong, C.M. Marcus and H. Dai, Science **286**, 263(1999).
[35] D.H. Cobden, *et.al.*, Phys. Rev. Lett. **81**, 681 (1998).
[36] H. Mehrez, J. Taylor, H. Guo, J. Wang, and C. Roland, Phys. Rev. Lett. **84**, 2682 (2000); H. Mehrez, H. Guo, J. Wang and C. Roland, Phys. Rev. B **63**, 245410 (2001).
[37] C. Roland, M.B. Nardelli, J. Wang, and H. Guo, Phys. Rev. Lett. **84**, 2921 (2000); C. Roland, M.B. Nardelli, H. Guo, H. Mehrez, J. Taylor, J. Wang, Y.D. Wei, Surf. Rev. Lett. **7**, 637 (2000).
[38] D. Orlikowski, H. Mehrez, J. Taylor, H. Guo, J. Wang, and C. Roland, Phys. Rev. B **63**, 155412 (2001).
[39] A.F. Andreev, Zh. Eksp. Teor. Fiz. **46**, 1823 (1964) [Sov. Phys. JETP **19**, 1228 (1964)].
[40] A. P. Jauho, N. S. Wingreen, and Y. Meir, Phys. Rev. B **50**, 5528 (1994).
[41] Q.F. Sun, J. Wang, T.H. Lin, Phys. Rev. B **58**, 13007 (1998); Phys. Rev. B **59**, 13126 (1999).
[42] B.G. Wang, J. Wang, and H. Guo, Phys. Rev. Lett. **82**, 398 (1999); J. Appl. Phys. **86**, 5094 (1999).
[43] We have omitted the factor of two for spin.
[44] T. Gramespacher and M. Buttiker, Phys. Rev. B **61**, 8125 (2000).
[45] J. Wang, Y.D. Wei, H. Guo, Q.F. Sun, and T.H. Lin, Phys. Rev. B **64**, 104508 (2001).
[46] Y. Nambu, Phys. Rev. 117, 648 (1960).
[47] Q.F. Sun, J. Wang, and T.H. Lin, Phys. Rev. B **59**, 3831 (1999).
[48] X. Blase et al, Phys. Rev. Lett. **72**, 1878 (1994); Y.A. Krotov et al, *ibid.* **78**, 4245 (1997); L. Chico, *et.al. ibid.* **76**, 971 (1996); V.H. Crespi et al, *ibid.* **79**, 2093 (1997); L. Chico et al, *ibid.* **81**, 1278 (1996); L. Chico et al, Phys. Rev. B **54**, 2600 (1996).
[49] M. Buongiorno Nardelli, Phys. Rev. B. **60**, 7828 (1999).
[50] Y.D. Wei, J. Wang, H. Guo, H. Mehrez, and C. Roland, Phys. Rev. B **63**, 195412 (2001).
[51] In fact, the barrier thickness and barrier height of armchair nanotube are larger than that of zigzag nanotube which favor the pumping of armchair nanotube. Yet the pumped current for zigzag nanotube is much larger than that of armchair nanotube with the same pumping amplitude.
[52] J. Wang and B.G. Wang, Phys. Rev. B **65**, 153311 (2002).

FIG. 1. Andreev reflection coefficient T_A as a function of Fermi energy for N-SWNT-S system (solid line) and transmission coefficient T as a function of Fermi energy for N-SWNT-N device (long dashed line). The SWNT is an armchair (5,5) metallic tube. Inset: a schematic plot of the molecular device.

FIG. 2. The pumped current I^{NS} versus Fermi energy for N-SWNT-S device at different pumping amplitudes: $V_p = 0.0014V$ (solid line), $V_p = 0.002V$ (dotted line) and $V_p = 0.005V$ (dashed line). Here long dashed line is the pumped current I^N versus Fermi Energy for the corresponding N-SWNT-N device (when $\Delta = 0$) at $V_p = 0.0014V$. The left inset: I^{NS}/I^N versus V_p at resonant point. The right inset: Andreev reflection coefficient T_A versus E_F with $V_p = 0.005V$ at different pumping moments: $t = 3\pi/4$ (solid line), $t = 0.95\times 3\pi/4$ (dotted line) and $t = 1.05\times 3\pi/4$ (dashed line).

FIG. 3. The pumped current I^{NS} versus Fermi Energy for N-SWNT-S device at different pumping amplitudes: $V_p = 0.001V$ (solid line), $V_p = 0.002V$ (dotted line) and $V_p = 0.005V$ (dashed line). The long dashed line is for the pumped current I^N versus Fermi Energy of the corresponding N-SWNT-N device at $V_p = 0.001V$. Here the SWNT is a zigzag (10,0) nanotube. The left inset: I^{NS}/I^N versus V_p at resonant point.

FIG. 4. The pumped current I^{NS} of the armchair SWNT as a function of pumping amplitude V_p at $E_F = 0$ (solid line). Other system parameters are the same as those in Fig.2. Dotted line is plotted according to $I = -1.06\times 10^4 V_p^2$. Inset: The pumped current I^{NS} of the zigzag SWNT as a function of pumping amplitude V_p at $E_F = 0$ (solid line). System parameters are the same as those in Fig.3. Dotted line is plotted according to $I = 8.3758\times 10^5 V_p^2$.

FIG. 5. The pumped current I^{NS} of the armchair SWNT as a function of phase difference ϕ at $E_F = 0$. Main figure: the weak pumping regime with $V_p = 0.0001V$ (solid line) and $V_p = 0.0002V$ (dotted line). Inset: the strong pumping regime with $V_p = 0.0014V$ (solid line), $V_p = 0.002V$ (dotted line), and $V_p = 0.005V$ (dashed line). Other system parameters are the same as those in Fig.2.

FIG. 6. The pumped current I^{NS} versus Fermi Energy for the N-SWNT-S device at different pumping amplitudes: $V_p = 1\times 10^{-6}V$ (solid line), $V_p = 2\times 10^{-6}V$ (dotted line). The long dashed line is the pumped current I^N versus Fermi Energy for the corresponding N-SWNT-N device at $V_p = 1\times 10^{-6}V$. The SWNT is a zigzag (10,0) nanotube with length L=92 layers. The upper inset: Andreev reflection coefficient T_A for N-SWNT-S device (solid line) and transmission coefficient T for the corresponding N-SWNT-N device (long dashed line). The lower inset: the amplified figure of a pumped current peak. The other system parameters: $\phi = \pi/2$ and $\Gamma_R = \Gamma_L = 0.0136eV$.

Fig.1

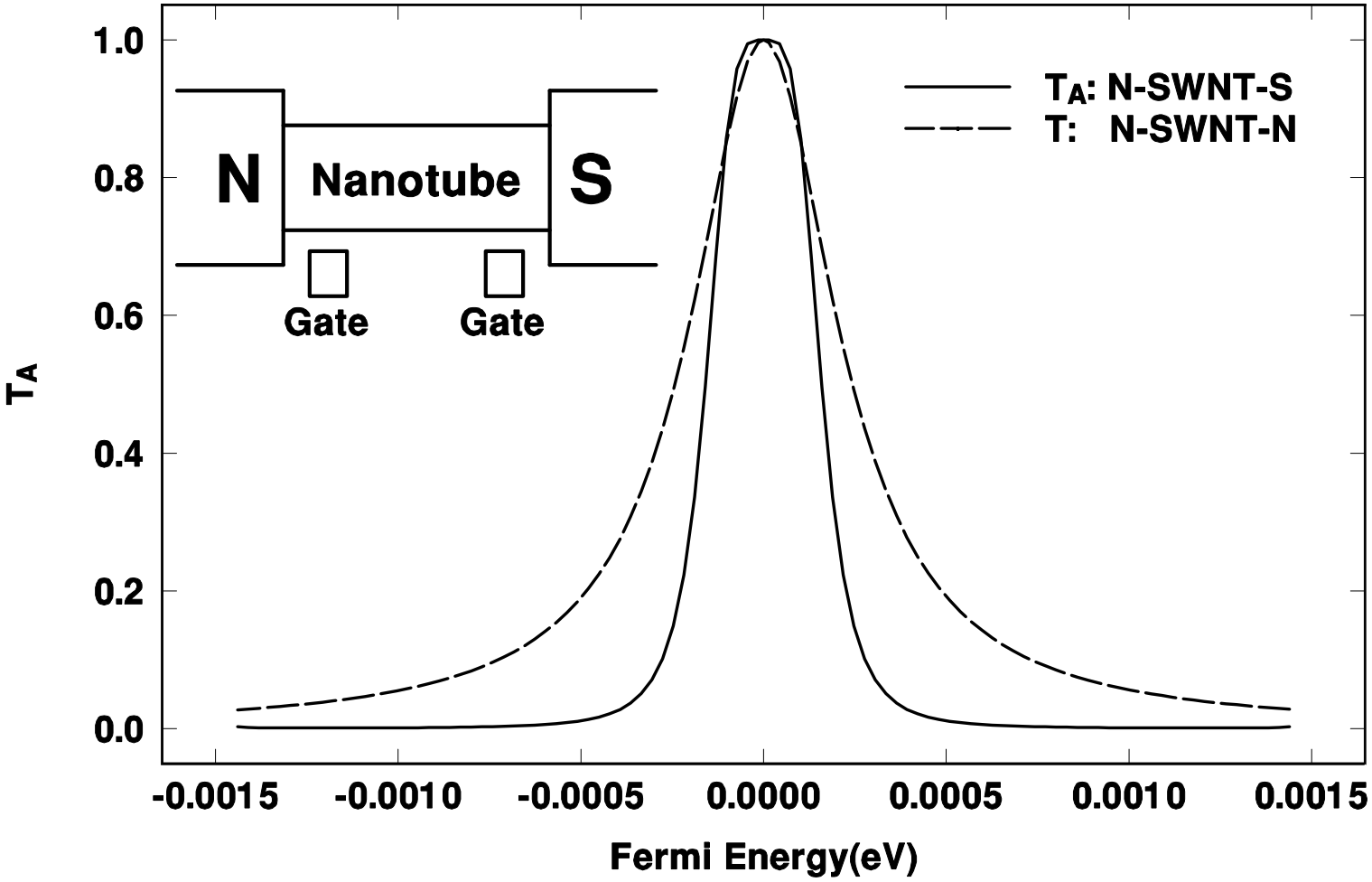
1.0
0.8
0.6
0.4
0.2
0.0
T_A
N
Nanotube
S
Gate
Gate
T_A: N-SWNT-S
T: N-SWNT-N
-0.0015
-0.0010
-0.0005
0.0000
0.0005
0.0010
0.0015
Fermi Energy(eV)

Fig.2

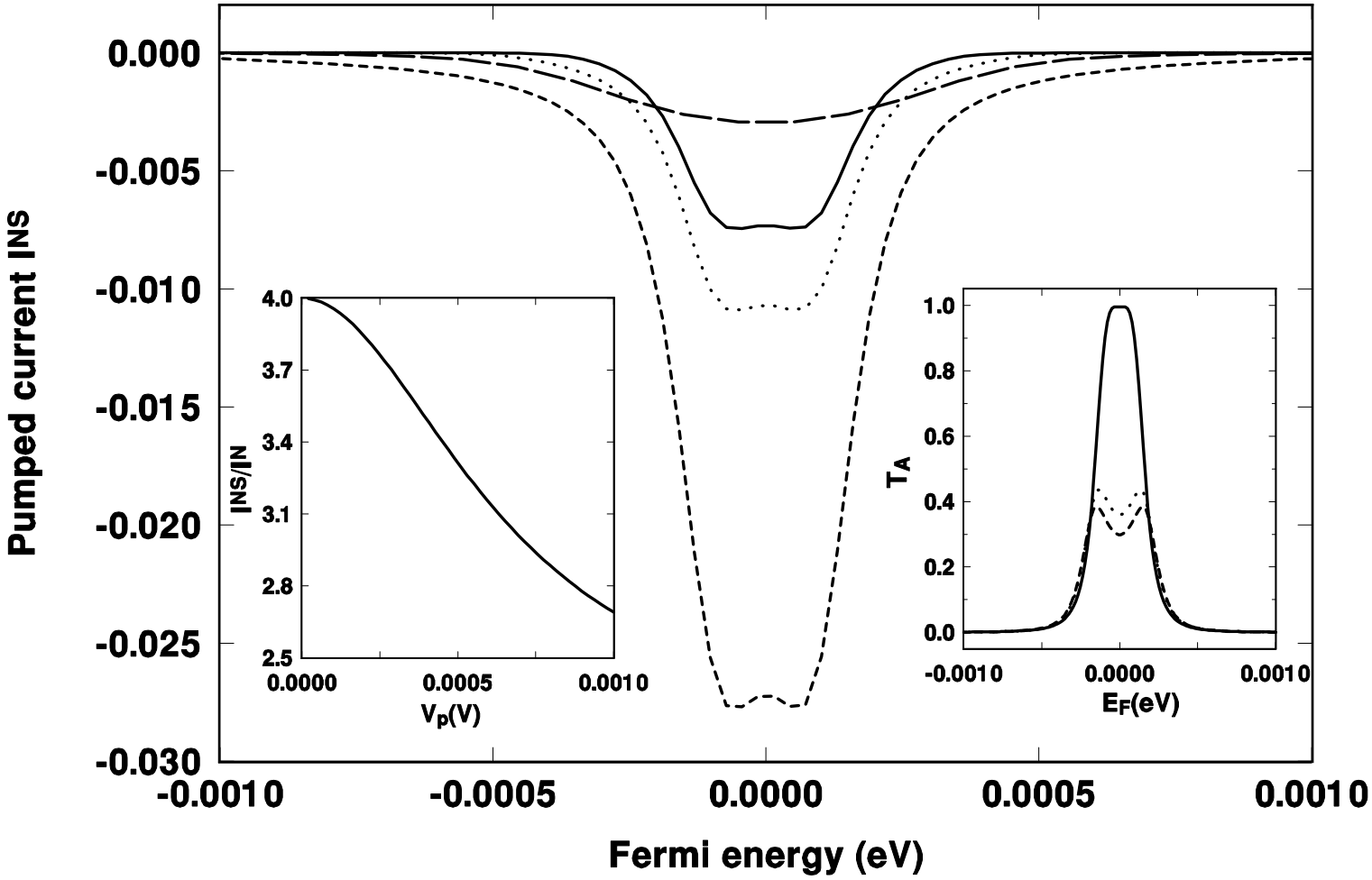
Pumped current INS
0.000
-0.005
-0.010
-0.015
-0.020
-0.025
-0.030
-0.0010
-0.0005
0.0000
0.0005
0.0010
Fermi energy (eV)
INS/IN
4.0
3.7
3.4
3.1
2.8
2.5
0.0000
0.0005
0.0010
Vp(V)
TA
1.0
0.8
0.6
0.4
0.2
0.0
-0.0010
0.0000
0.0010
EF(eV)

Fig.3

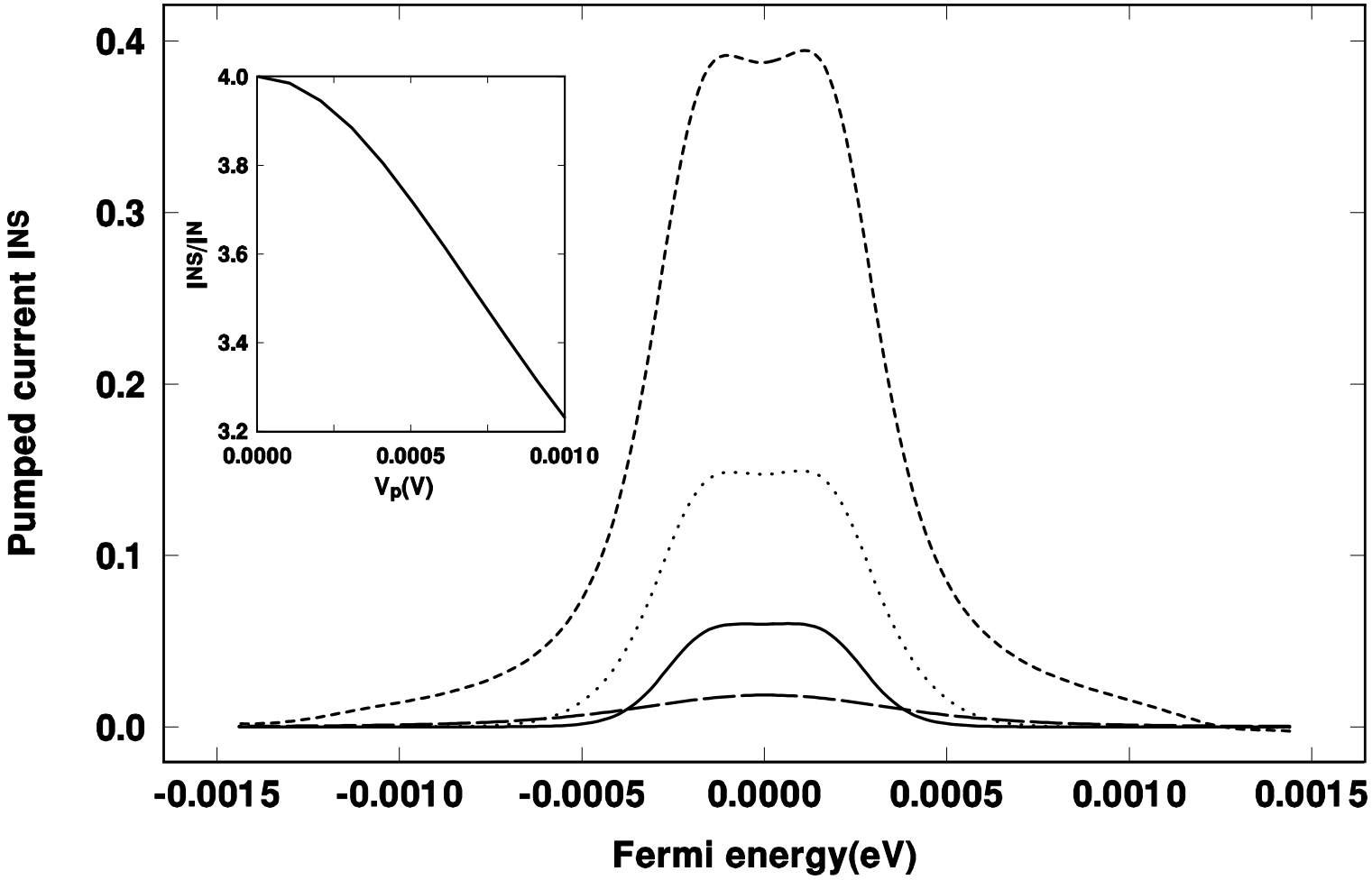
Pumped current INs
0.4
0.3
0.2
0.1
0.0
-0.0015
-0.0010
-0.0005
0.0000
0.0005
0.0010
0.0015
Fermi energy(eV)
INS/IN
4.0
3.8
3.6
3.4
3.2
0.0000
0.0005
0.0010
Vp(V)

Fig.4

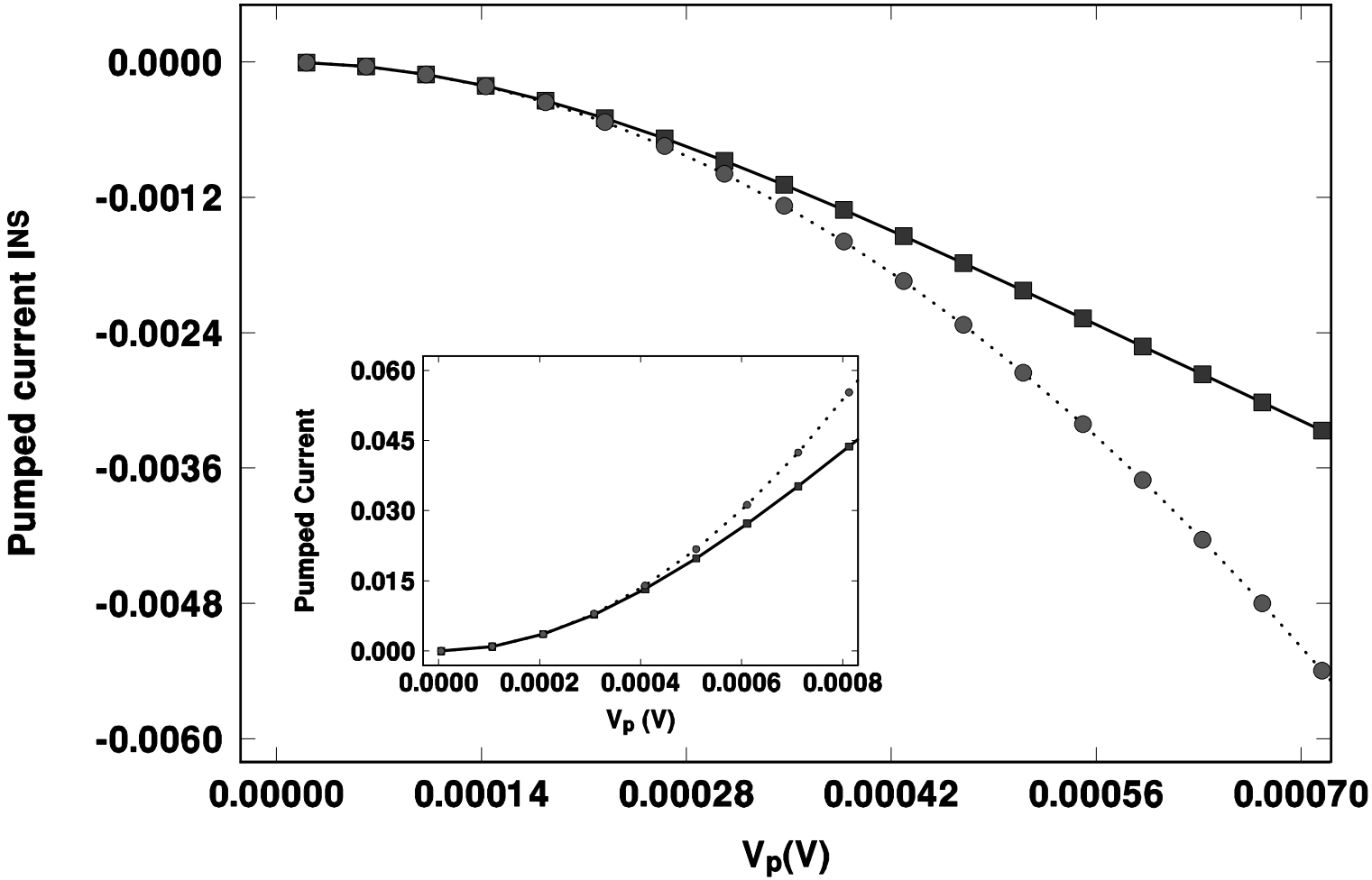
Pumped current INs
0.0000
-0.0012
-0.0024
-0.0036
-0.0048
-0.0060
0.00000
0.00014
0.00028
0.00042
0.00056
0.00070
Vp(V)
Pumped Current
0.060
0.045
0.030
0.015
0.000
0.0000
0.0002
0.0004
0.0006
0.0008
Vp (V)

Fig.5

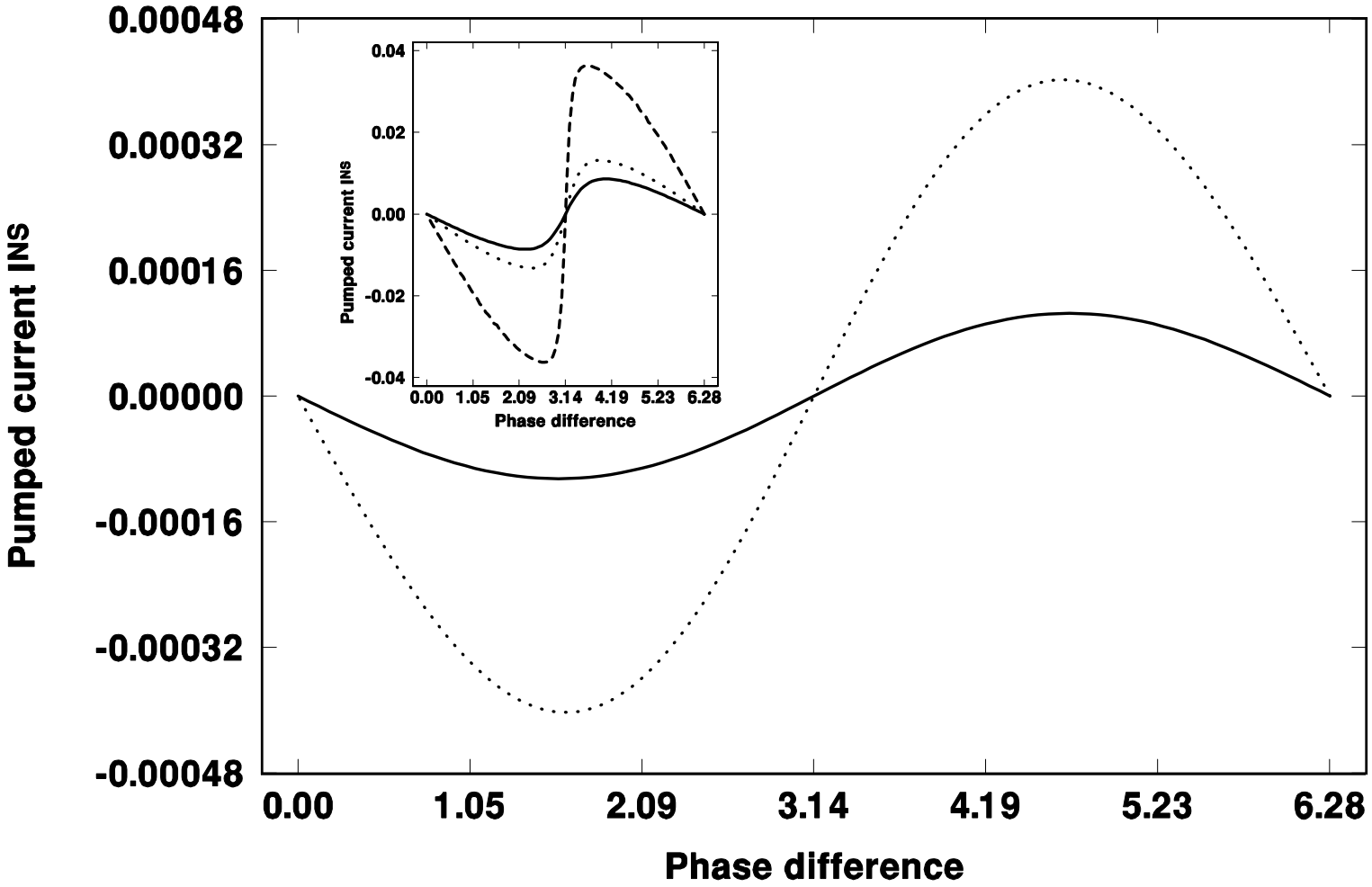
0.00048
0.00032
0.00016
0.00000
-0.00016
-0.00032
-0.00048
Pumped current INS
0.00
1.05
2.09
3.14
4.19
5.23
6.28
Phase difference
0.04
0.02
0.00
-0.02
-0.04
Pumped current INS
0.00 1.05 2.09 3.14 4.19 5.23 6.28
Phase difference

Fig.6

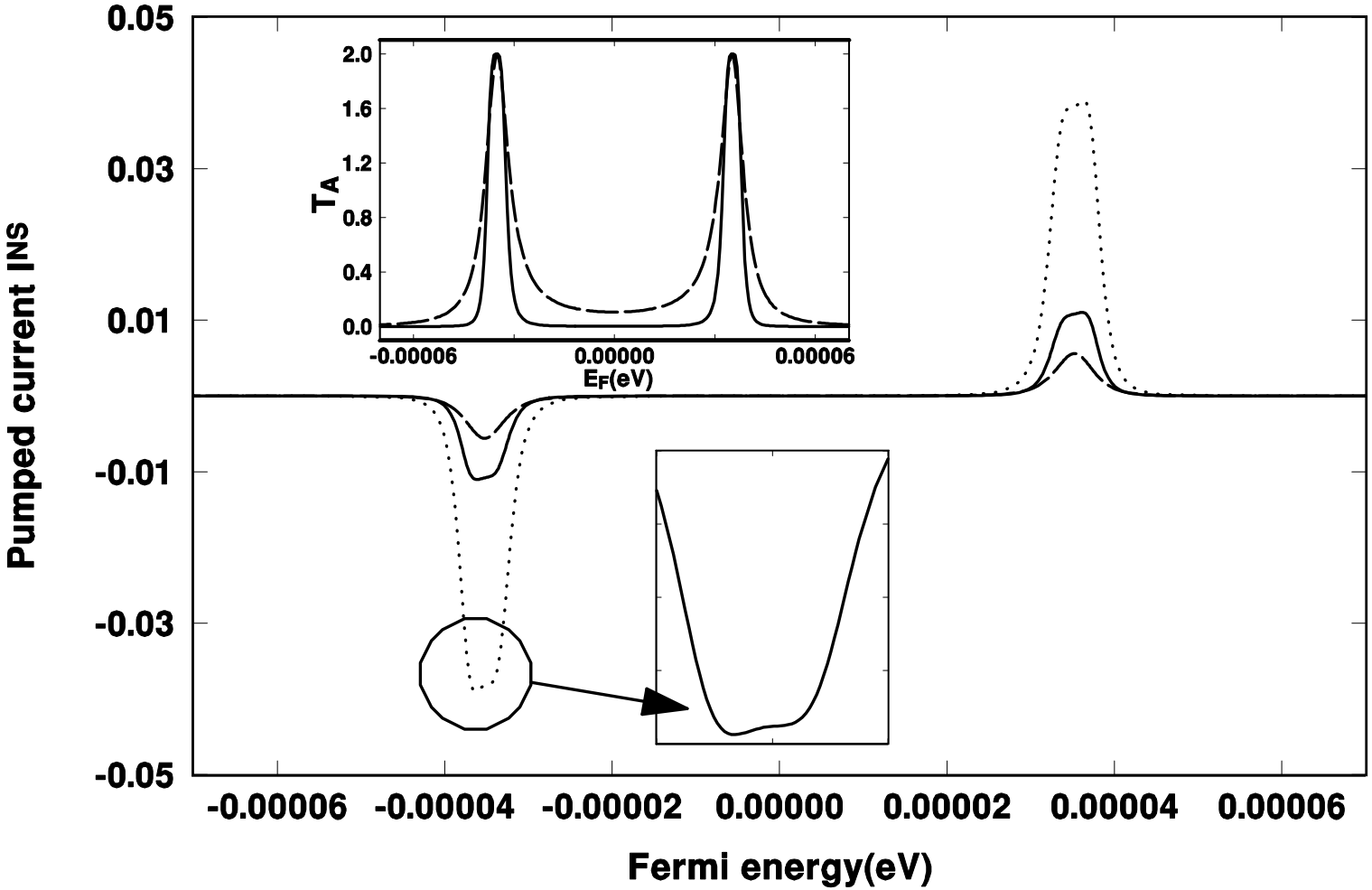
Pumped current INS
0.05
0.03
0.01
-0.01
-0.03
-0.05
-0.00006
-0.00004
-0.00002
0.00000
0.00002
0.00004
0.00006
Fermi energy(eV)
T_A
2.0
1.6
1.2
0.8
0.4
0.0
-0.00006
0.00000
0.00006
E_F(eV)